

Open-Set Object Recognition Using Mechanical Properties During Interaction

Pakorn Uttayopas, Xiaoxiao Cheng and Etienne Burdet

Abstract—Current robotic haptic object recognition...

Index Terms—open-set setting, haptic exploration, supervised learning for classification, unsupervised learning for clustering.

I. INTRODUCTION

Robots become more common to operate in household environments surrounded by various kinds of objects. When vision is unavailable, tactile perception helps robots interact with such an environment more effectively [1]. However, most of the existing work was done in a close-set condition in which testing objects always belong to one of the objects in the training set [2]–[5]. This is different from the open-set condition where testing objects can be beyond the knowledge of the robots. This may cause robots to fail in recognising objects and, consequently, in object manipulation.

Humans, on the other hand, can easily handle novel objects in open-set conditions by learning and gathering new information from the exploration process and updating their knowledge. For robots to handle such a situation, a concept of open-set recognition (OSR) has been proposed as the first step for robots to interact with novel objects [6]. Unlike traditional close-set recognition, OSR enables robots to classify the samples of known objects and also detect samples of novel objects which are collected and investigated to gain further information.

Previous works show that OSR has been successfully applied in various fields such as object detection [7]–[9], face recognition [10]–[12], and autonomous driving [13]. However, these systems are not able to incrementally learn new information from novel objects and label them. This could be addressed by involving humans to assign specific labels to novel objects or by implementing semi-supervised learning in the recognition system for incremental automatic labeling [14]. The simplest method might be to apply unsupervised learning methods after finishing the novelty detection [15].

While OSR has been widely applied in the field of vision [16], it is rarely seen in tactile-based applications. Liu et al. [17] introduced, for the first time, the robotic material recognition system for open-set conditions. The framework deployed a Generative Adversarial Network (GAN) to generate fake novel tactile images as an example used in prototype-based learning [18] to prepare for novelty detection. However, the system does not specifically label the detected novel objects

and requires a lot of tactile images to learn. Besides, the values of tactile information can be affected by interactions, causing confusion among materials.

Unlike tactile information, mechanical properties such as coefficient of restitution, viscoelasticity, and friction coefficient provide a unique representation of objects [19]–[21] and are well distinguishable among objects [22]–[24]. Inspired by these properties, we proposed a simple open-set tactile recognition framework that uses objects' mechanical properties to perform classification for known objects and clustering for novel objects. The classification can be done by a supervisor learning method while a distance-based unsupervised learning method is used for clustering.

Since the mechanical properties of novel objects cannot be observed during training, we exploit knowledge of known objects to estimate the new cluster's centre and size via a regression model, as this approach was used to generate samples in zero-shot learning methods [25]. This is intended to enable the framework to cluster novel objects online, without a complete set of samples. Furthermore, it also aims to make the new cluster as close as the ground truth cluster, unlike general clustering algorithms where the initial cluster's centre is randomly selected.

In this paper, we extend the framework in [24] that estimates mechanical properties during interaction to be able to perform open-set recognition and incrementally label novel objects. The framework is validated using the estimated mechanical properties collected in [24]. Our results are compared with alternative methods used to deal with open-set conditions. Lastly, the role of the framework's hyperparameter on novel object clustering results is investigated.

II. OBJECT RECOGNITION FRAMEWORK

A. Problem Statement

In the problem that we investigate, a robot is trained to recognise the set of objects class $Y = \{y_1, y_2, \dots, N\}$ from mechanical properties and test it on the set $O = Y \cup Z$ containing the known classes Y and novel classes Z (unlabelled), s.t. $Y \cap Z = \emptyset$ and $Y \neq Z$. T. During the training phase, a robot learns parameters from a training dataset $D_{train} = \{(y_i, (x_1, \dots, x_{TN}))\}_{i=1}^N$, where TN is the number of the training sample and x represents the mechanical properties collected from a certain space X . During the test phase, a test sample $x \in X$ is either classified as one of the known classes or discovered as a novel class and clustered accordingly. This allows the number of clusters of novel objects to grow as a new class is discovered $U = \{u_1, u_2, \dots, L\}$. We assume that

Department of Bioengineering, Imperial College of Science, Technology and Medicine, London, UK. {pu18, xcheng4, e.burdet}@imperial.ac.uk.

Corresponding authors: Pakorn Uttayopas, Xiaoxiao Cheng.

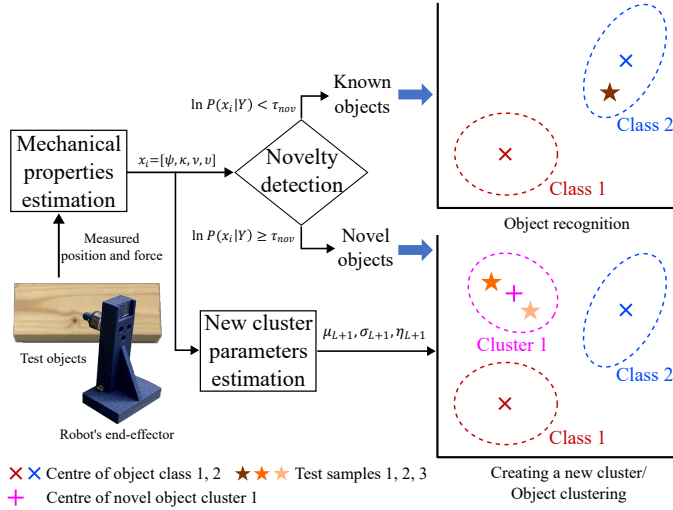


Fig. 1. Object recognition and clustering process. The end-effector force and position measured during the interaction process are used to obtain mechanical properties with an estimator. The estimated mechanical features are then used as a test sample x_i to identify as either known or novel objects. Test sample 1 is one of the known objects, thus the classification is performed. Test sample 2 is a novel object, thus cluster 1 is generated by estimating its parameters. However, test sample 3 is also a novel object, but it is labeled as cluster 1 because it lies in the cluster boundary.

the robot does not have any prior knowledge of whether the test sample belongs to known classes or unlabelled classes and only knows the number of known classes.

B. Framework Overview

Fig. 1 shows the proposed framework with its two components; mechanical properties estimation, and recognition/clustering. A robot interacts haptically with a test object to retrieve interaction force at different positions to estimate an object's mechanical properties such as coefficient of restitution ψ , stiffness κ , viscosity ν , and friction coefficient v via the dual Kalman filter technique [24]. These estimated mechanical properties are used as a test sample x_i to either recognise the known objects or label them as novel objects depending on the novelty detection.

The novelty detection is based on the probability density function of x_i given the training mechanical properties. This reflects how likely x_i belongs to one of the known object classes. Specifically, we calculate a log-likelihood of x_i across all the known classes $\ln p(x_i|Y)$ based on classes' Gaussian parameters. We determine whether the test sample belongs to one of the known classes or the novel class as follows

$$c = \begin{cases} \arg \max_{y \in Y} p(y|x_i), & \ln p(x_i|Y) < \tau_{nov} \\ novel, & \text{otherwise} \end{cases} \quad (1)$$

where τ_{nov} is a novelty threshold, and $p(y|x_i)$ is the posterior of a known object's class y given x_i calculated from the Naive Bayes classifier.

For novel classes, a distance-based clustering method is used to decide which cluster of x_i belongs. In brief, x_i is labeled as the same class as the closest existing cluster that x_i lies within its boundary η_c . If x does not lie in any of the

existing cluster boundaries, the new cluster is created. This is done by estimating parameters describing the new cluster such as the centre point and its boundary via a regression model from the training dataset (details in section III).

Since novel clusters are synthetically created, their parameters need to be updated with the real sample. This is done once the number of datapoints within clusters reaches a particular number τ_{update} . After all datapoints are fed, sample points that lie within the cluster having the number of datapoints lower than τ_{out} are treated as outliers and removed from the framework.

III. CLUSTERING ALGORITHM

A. Labelling the test sample

As x_i is identified as a novel object, it could belong to the existing cluster of novel objects. The probability of x_i belonging to an existing cluster is calculated based on a distance

$$p(u|x_i) = \frac{\exp(-\frac{1}{2} d_M(x_i, \mu_u))}{\sum_{u'=1}^L \exp(-\frac{1}{2} d_M(x_i, \mu_{u'}))} \quad (2)$$

where μ_u is mean values of each mechanical properties in cluster u , and $d_M(x_i, \mu_u)$ is the Mahalanobis distance between x_i and a cluster centre μ_u considering the cluster covariance Σ_u

$$d_M(x_i, \mu_u) = (x_i - \mu_u)^\top \Sigma_u^{-1} (x_i - \mu_u). \quad (3)$$

The label could be assigned as

$$c = \arg \max_{u \in U} p(u|x_i). \quad (4)$$

However, if x_i lies beyond the boundary of the most probable cluster, it is discovered as a sample in a new cluster. The new cluster is created and the number of clusters is increased by 1. The final assigned label is given by

$$c = \begin{cases} c, & d_M(x_i, \mu_c) \leq \eta_c \\ N + L + 1, & \text{otherwise} \end{cases} \quad (5)$$

where η_c is the boundary of the most probable cluster c , the longest Mahalanobis distance between its points and center.

B. Learning the regression model

As a new cluster is discovered, a regression model is exploited for its ability to predict the cluster parameters without any knowledge of the novel object. The relationship between the feature vector a_y and its cluster parameters θ_y for each class y can be defined as $\theta_y = f_\theta(a_y)$ where f_θ is a mapping function and could consist of multiple functions depending on the number of parameters in θ_y .

We define θ_y as the mean vector $\mu_y \in \mathbb{R}^D$ and covariance matrix $\Sigma_y \in \mathbb{R}^{D \times D}$ in D dimensional Gaussian distribution and assume that $\Sigma_y = \text{diag}(\sigma_y^2)$ where $\sigma_y^2 = [\sigma_{y,1}^2, \dots, \sigma_{y,D}^2]$ for simplification. The parameters μ_y and σ_y^2 can be modelled as linear functions of mechanical properties vector a_y :

$$\mu_y = \mathbf{W}_\mu a_y, \quad y = 1, \dots, N \quad (6)$$

$$\sigma_y^2 = \mathbf{W}_{\sigma^2} a_y, \quad y = 1, \dots, N \quad (7)$$

where $\mathbf{W} \in \mathbb{R}^{D \times K}$ is the output weight matrix and its subscript indicates which parameters it belongs to.

The least-squares technique with Tikhonov regularisation is applied to match an estimation of μ_y and σ_y^2 with the training data. We denote $\mathbf{M} = [\mu_1, \dots, \mu_M] \in \mathbb{R}^{D \times M}$, $\mathbf{R} = [\sigma_1^2, \dots, \sigma_M^2] \in \mathbb{R}^{D \times M}$, $\mathbf{A} = [a_1, \dots, a_M] \in \mathbb{R}^{K \times M}$, thus \mathbf{W} is estimated as follows

$$\hat{\mathbf{W}}_\mu = \mathbf{M}\mathbf{A}^\top (\mathbf{A}\mathbf{A}^\top + \lambda_\mu \mathbf{I})^{-1} \quad (8)$$

$$\hat{\mathbf{W}}_{\sigma^2} = \mathbf{R}\mathbf{A}^\top (\mathbf{A}\mathbf{A}^\top + \lambda_{\sigma^2} \mathbf{I})^{-1} \quad (9)$$

where λ is the regularisation parameter which is used to prevent overfitting to the training data, and \mathbf{I} is the identity matrix.

Inspiring by the next-generation reservoir computing [26], the feature vector is composed of a linear and nonlinear part of the feature $a_y = a_{lin,y} \oplus a_{nonlin,y}$ where \oplus is the vector concatenation. The mechanical properties are the main attributes used in the framework, the linear feature is $a_{lin,y} = [\kappa, \nu, \psi, v]^\top$ and the quadratic polynomial function was applied on $a_{lin,y}$ to obtain nonlinear part of feature vector as $a_{nonlin,y} = [\kappa^2, \kappa \cdot \nu, \dots, \nu^2, \nu \cdot \psi, \dots, \psi \cdot v, v^2]^\top$. Totalling, a_y contains 14 features and each known object class has TN datapoints, the feature vector becomes $a_y = [a_{y,1}, \dots, a_{y,TN}]$, thus $D = 4$, $K = 14$ and $M = N \cdot TN$.

C. Creating a new cluster

Given the estimated weight $\hat{\mathbf{W}}_\mu$ and $\hat{\mathbf{W}}_{\sigma^2}$, parameters describing the new cluster can be calculated as follows

$$\mu_{L+1} = (1 - \alpha) \hat{\mathbf{W}}_\mu a_{x_i} + \alpha x_i \quad (10)$$

$$\sigma_{L+1}^2 = \beta \hat{\mathbf{W}}_{\sigma^2} a_{x_i} \quad (11)$$

where $\alpha \in [0, 1]$ is a hyperparameter indicating centre position ($\alpha = 0$: the predicted mean as centre and $\alpha = 1$: the test sample x_i as centre) and $\beta \in [0, \infty)$ is a hyperparameter indicating boundary of cluster (higher β results in larger boundary).

To define cluster boundary, eq. (3) is calculated based on N_{gen} points of generated datapoints $X_{gen} \sim \mathcal{N}(\mu, \sigma^2)$ to search for the longest distance from X_{gen} to the centre. All parameters of the cluster are updated once the number of datapoints reaches the threshold τ_{update} . Note that X_{gen} is included to update the parameters with the test datapoints.

IV. EXPERIMENTAL SETUP

A. Data collecting

To test the developed object recognition and clustering framework, it was applied to mechanical properties data collected in [24]. The HMan robot [27] (shown in Fig. 2a) was used to estimate object mechanical properties through robot-object interactions. This robot is a 2-DOF cable-driven planar robot controlled by two actuators (model 352699; Maxon Motor). These actuators were operated by the NI real-time system with a 1 kHz sampling rate. A finger equipped with a six-axis force sensor (SI-25-0.25; ATI Industrial Automation) was installed on the base of the robot's end-effector to measure

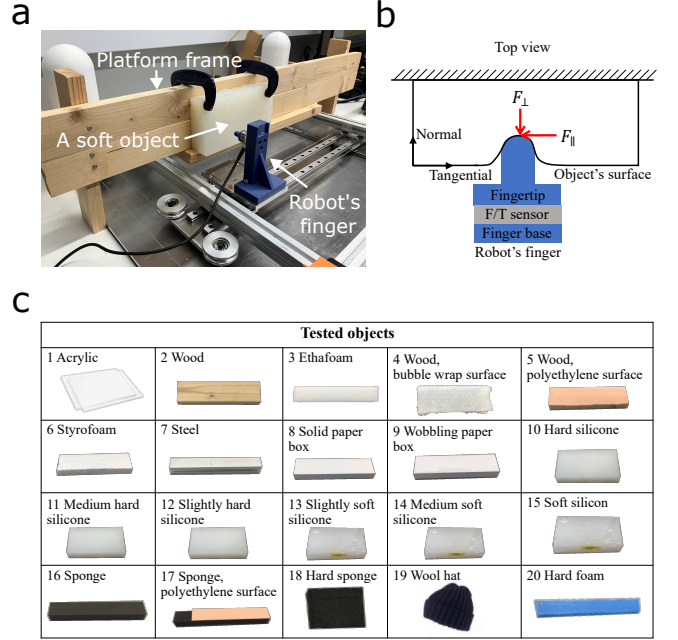


Fig. 2. Experimental setup. (a) HMan robot with a sensorized finger and an object to examine. A wooden platform frame is used to attach various objects for the robot to explore. The finger is driven by two motors in the normal and tangential directions to the object's surface. (b) Diagram of robot finger interacting with an object's surface. (c) 20 objects used in the experiment.

forces during robot-object interaction with a 1 kHz sampling rate.

The mechanical properties estimator [24] was implemented on the robot to estimate the coefficient of restitution, stiffness, viscosity, and friction coefficient of 20 objects (see Fig. 2c). The estimation was done with interactions as follows

- **tapping**: To estimate the coefficient of restitution, a constant force was exerted on the robot's end-effector for 0.5 seconds followed by its free movement toward the object's surface to create an impulse.
- **indentation**: To estimate the surface viscoelasticity, the robot pressed its finger against the object's surface in the normal direction with a desired trajectory $r_\perp = 0.01 \sin(8t) + 0.01 \text{ m}$, $t \in (0, 20] \text{ s}$.
- **sliding**: To estimate the coefficient of friction, the robot moved its finger in the tangential direction on the object's surface with a constant velocity of 0.04 m/s while maintaining a constant normal force of 4 N.

These interactions were performed separately which allowed the robot to interact with objects smoothly and to have sufficient contact with the objects' surfaces. The estimation was repeated 25 times for each pair of actions and object.

B. Data processing

A dataset was formed based on the estimated mechanical properties. The coefficient of restitution was directly used as one of the features. The mean values of stiffness, viscosity, and friction coefficient for the last two seconds of estimation

were extracted as the steady-state values and used as additional features.

We assumed that the robot does not have any knowledge of some object classes, thereby the dataset was split into two sets of classes; known classes and novel classes. We randomly selected 12 classes (60% of the number of classes) to be known classes and the remaining 8 classes (40% of the number of classes) to be novel classes. 3/4 datapoints in the known class were randomly selected and used to learn object recognition parameters and regression model weights. On the other hand, the remaining 1/4 datapoints were used as the testing set combined with the set of novel classes. To ensure the robustness of the framework, the evaluation was done with 25 repetitions with different choices of known classes and novel classes each.

C. Alternative algorithms

Given the problem stated in section II-A, there are rarely ready-to-use baselines, especially in the context of haptic, that we can compare with our framework. Thus, we extended the existing novelty detection, supervised learning, and unsupervised learning methods as alternative methods to compare with our results in three tasks: 1.) how well it can distinguish between known and novel objects (novelty detection), 2.) how well it can recognise the known object (known object classification), and 3.) how well it can label novel objects (novel object clustering).

In the first task, we compare our novelty detection results with three alternative methods: {Isolated forest, Gaussian Mixture Models, and a Nearest Non-Outlier algorithm (NNO) [6]}. An isolated forest algorithm is similar to a random forest algorithm, but it is used to detect anomalies by searching for boundaries between anomalies and normal datapoints. GMM was proposed as a novelty detector in [28]. It detected anomalies by comparing the log-likelihood of the fitted GMM given the test sample to a threshold. If the value is lower than the threshold, the test sample is novel. Lastly, the NNO is a distance-based classifier with the ability to detect anomalies. A distance function of a test sample. If the distance function value is lower than 0, the test sample is novel.

In the second task, the test datapoints that are identified as known objects by the isolated forest and GMM will be classified using the same Naive Bayes classifier (NB) as our framework. On the other hand, the identified test datapoints as known objects from the NNO are classified by the nearest class mean classifier (NCM) [29] as the NCM is already integrated with the NNO algorithm. Lastly, we replace our classifier in the framework with another two alternative classifiers {a fully connected neural network (NN) and a polynomial-kernel support vector machine (SVM)} to compare classification results from them.

In the third task, four alternative clustering algorithms {K-means, Incremental online k-means (IOKM) [30], DBscan, and DenStream [31]} are used to label test datapoints identified as novel objects by our novelty detector. Both K-means and IOKM are centroid-based clustering methods, but the latter is an online version of K-means. On the other hand, DBscan is a

density-based clustering method that clusters areas with high density separately from low-density areas. It does not require a pre-defined number of clusters, unlike the first two algorithms. DenStream is the extension of DBscan that could work online. All alternative algorithms do not have the estimators to predict cluster centres and boundaries.

We also compare our new cluster parameters estimator with two alternative methods: {random and variational autoencoder (VAE)}. For random, the new cluster centre and boundary are randomly generated. On the other hand, VAE is used to generate cloud points of novel objects based on the test datapoints. These cloud points then are used to calculate the new cluster centre and boundary.

D. Evaluation metrics

The accuracy of known/novel object distinction in the first task and the known object recognition rate in the second task can be reported as the proportion of the number of datapoints recognised or identified correctly and the total number of datapoints.

To evaluate clustering results in the third task, we compared the results of assigned labels (clustering results) of the novel objects with the true labels using the adjusted rand index (ARI):

$$\text{ARI} = \frac{\sum_{ij} \binom{n_{ij}}{2} - \left[\sum_i \binom{a_i}{2} \sum_j \binom{b_j}{2} \right] / \binom{n}{2}}{\frac{1}{2} \left[\sum_i \binom{a_i}{2} + \sum_j \binom{b_j}{2} \right] - \left[\sum_i \binom{a_i}{2} \sum_j \binom{b_j}{2} \right] / \binom{n}{2}} \quad (12)$$

where n_{ij} is the number of datapoints in a cluster of known label A_i and a cluster of assigned label B_j , a_i and b_j is the number of datapoints in cluster A_i and B_i respectively.

The ARI evaluates the similarity between a set of assigned labels and the true labels in a range of $[-1, 1]$, where $\text{ARI} < 0$ means the clusters are worse than the results generated randomly and $\text{ARI} = 1$ means the cluster is perfectly matched with known labels.

V. EXPERIMENTAL RESULTS

A. Novelty detection

Table I shows that our novelty detector yields the highest overall correction at 91% and the highest recognition rate of identifying known objects as known objects at 95%. For detecting novel objects, our method could reach 89% correction which is higher than Isolated forest and GMM results (80% and 84% respectively), but it is lower than NNO results which is 96%. However, NNO only provides a 72% accuracy for identifying known objects which is the lowest value. This shows that our method could maintain a relatively high recognition rate in both identifying known objects and detecting novel objects.

B. Multiclass classification of known objects

The classification results of known objects are shown in Table II. A recognition rate of 95% was achieved when the Naive Bayes classifier was used to classify identified known

TABLE I
ACCURACY OF NOVELTY DETECTION: DISTINCTION BETWEEN KNOWN AND NOVEL OBJECTS

Methods	Accuracy (%)		
	Known	Novel	Overall
Isolated Forest	88.19 ± 5.91	80.76 ± 9.93	82.79 ± 7.00
GMM [28]	88.28 ± 6.21	84.69 ± 5.38	86.64 ± 3.55
NNO [6]	72.29 ± 9.26	96.28 ± 2.50	90.36 ± 3.27
Our	95.76 ± 1.87	89.21 ± 4.76	91.06 ± 2.98

objects from the novelty detector. The results were slightly higher than other classifiers such as NN and SVM which is around 94% recognition rate. On the other hand, using other novelty detectors such as Isolated forest and GMM with the same Naive Bayes classifier provided recognition rates around 85 – 88%. Lastly, NNO yielded a 91% recognition rate. These results show that the Naive Bayes classifier provided the highest recognition.

TABLE II
RECOGNITION RATE FOR MULTICLASS CLASSIFICATION OF KNOWN OBJECTS

Method	Recognition rate (%)
Isolated forest+NB	85.73 ± 6.41
GMM+NB	88.13 ± 4.38
NNO [6]	91.36 ± 3.41
Our, but NN	94.16 ± 1.85
Our, but SVM	93.78 ± 1.96
Our	95.58 ± 1.61

C. Clustering of novel objects

Table III shows that our clustering algorithm could achieve values of ARI at 0.70. The K-means-based algorithm yields values of 0.60 – 0.64 ARI. On the other hand, the DBscan-based algorithm provided a lower ARI at 0.64 – 0.66. Using VAE as a new cluster parameters estimator resulted in the lowest value of ARI at almost 0. This result is even lower than the framework that randomly generates cluster parameters. These results show that our clustering algorithm outperforms other methods. Besides, using a regression model to estimate cluster parameters yields better results than using random parameters and VAE.

TABLE III
EVALUATION OF CLUSTERING RESULTS FOR NOVEL OBJECTS

Method	ARI
K-means	0.642 ± 0.123
IOKM [30]	0.604 ± 0.078
DBscan	0.667 ± 0.135
DenStream [31]	0.646 ± 0.082
Our, but random	0.120 ± 0.025
Our, but VAE	0.001 ± 0.002
Our	0.701 ± 0.096

D. Clustering results with various novel classes threshold

We investigated the performance of our clustering algorithms when the number of novel classes varied from 10 to

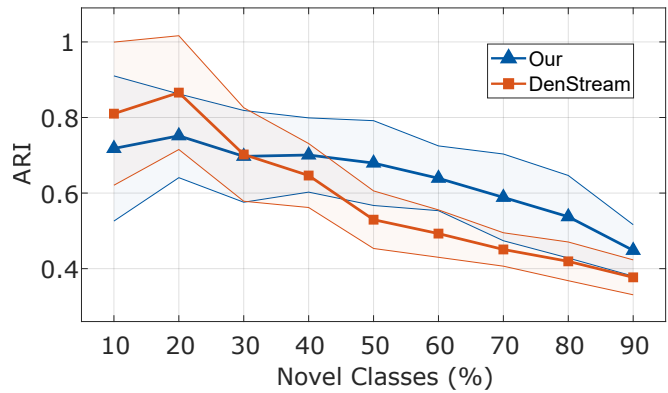


Fig. 3. Performance’s comparison of different algorithms to recognise objects with different posterior thresholds showing mean values of ARI and their standard deviation.

90% of the total classes in the testing set. We also compared our results with the DenStream results where both algorithms are online algorithms and do not require the number of clusters.

Fig. 3 shows that mean values of the ARI in both algorithms expectedly decreased with more novel classes in the testing set. Our clustering algorithm could achieve an ARI of 0.72 at 10% novel classes and gradually decrease to 0.45 at 90% novel classes. On the other hand, DenStream provided an ARI of 0.81 at 10% of novel classes before the value decreased to 0.37 at 90% of novel classes.

The results demonstrated that our algorithm is less sensitive than the DenStream when the number of novel classes is increased. In fact, our algorithm provides higher values of ARI than the DenStream in 40-90% of novel classes. Both algorithms provide similar values of ARI which is 0.7 at 30% novel classes. However, DenStream provides higher values of ARI than our results in the range of the novel classes 10-20%.

VI. HYPERPARAMETERS STUDIES

To investigate the effect of hyperparameters on clustering results, the values of α , β , N_{gen} in the cluster estimator and the updating threshold τ_{update} were varied. Each hyperparameter is evaluated with the 40% of novel classes in the testing set and is reported by calculating the ARI using eq.12.

A. Hyperparameters in the new cluster estimator

The first hyperparameters in the new cluster estimator α control the location of the new cluster centre. Fig. 4a shows that the mean value of the ARI increases from 0.62 at $\alpha = 0$ to 0.70 at $\alpha = 0.4$. Following this, all values of α above 0.4 have shown similar performance. These results suggest that the predicted mean from the new cluster estimator may not be accurate enough to use as the centre of the new cluster. However, shifting it to be close to the test sample helps improve the cluster results as the test sample is obtained from the real objects.

The β controls the standard deviation of datapoints inside the new cluster. Fig. 4b shows mean values of the ARI obtained when the β is varied from 1 to 4. Changes in the

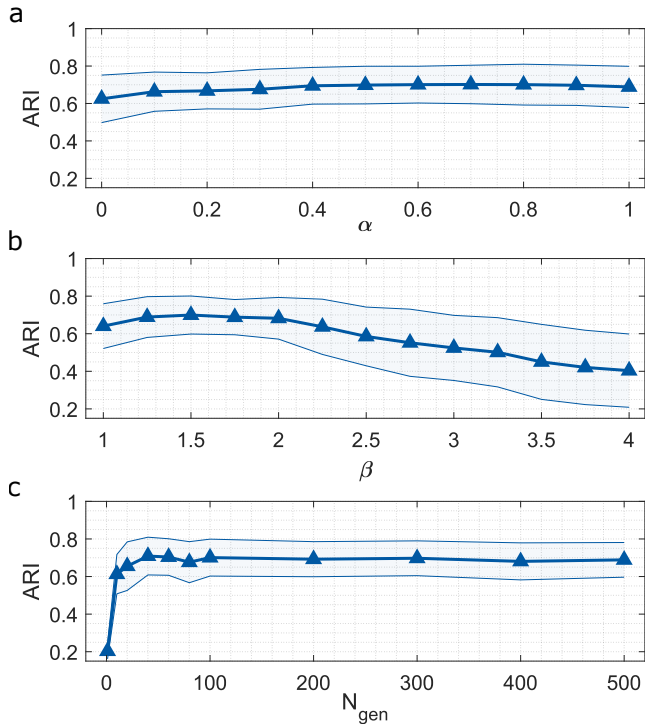


Fig. 4. The mean values of ARI and its standard deviation obtained using different values of (a) α , (b) β , and (c) N_{gen} in the new cluster estimator.

ARI are observed as the ARI is 0.64 at $\beta = 1$ and then the value increases until reaching its peak which is 0.70 at $\beta = 1.5$. This is followed by the reduction of ARI as the β increases. These results suggest β needs to be sufficiently large enough for test datapoints to lie in the correct cluster, but not too large that all datapoints lie in the same cluster.

Lastly, N_{gen} defines the number of datapoints used to find the boundary parameter η_c . Fig. 4c shows that the ARI increases from 0.20 at $N_{gen} = 1$ to reach its saturated point which is 0.70 at $N_{gen} = 40$. These results suggest that a small N_{gen} may generate datapoints that are close to the cluster centre, thus the calculated boundary may be smaller than it is supported to be. A larger N_{gen} may guarantee the correct boundary of the new cluster. However, too large N_{gen} can cause a higher computational cost as more datapoints need to be calculated.

B. Updating threshold for novel object clusters

The τ_{update} defines when the new cluster parameters should be updated as the new datapoints are assigned to the cluster. Fig. 5 illustrates that the values of ARI change from 0.96 to 0.6 when 5 new datapoints are fed at the beginning. However, the ARI starts to increase as more datapoints are added to the system until it reaches its saturation point depending on values of τ_{update} .

ARI yield values of 0.68-0.69 in the range of 1 to 10 for τ_{update} , especially in the latter number of fed datapoints. These results suggest that updating parameters frequently could lead to slightly poor clustering results. When τ_{update} increases, the ARI also slightly increases. However, the ARI reaches its saturation at 0.71 after τ_{update} reaches 15. These results

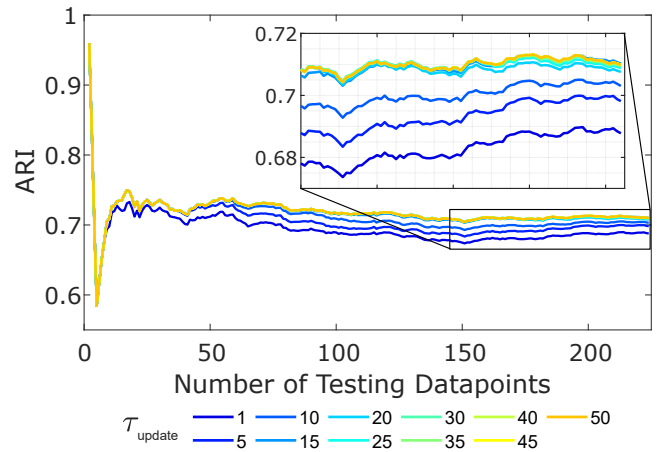


Fig. 5. Performance's comparison of different values of τ_{update} showing the evolution of the mean values of ARI as a function of the number of testing datapoints.

suggest that updating parameters when there are 15 new datapoints in the cluster is the balanced choice of update for this dataset.

VII. DISCUSSION

This paper introduced an open-set recognition framework based on the estimation of mechanical properties. This method extends the recognition framework in [24] to identify known objects and also to incrementally learn novel objects online. The algorithm's viability was demonstrated in simulation using the mechanical properties estimated from real objects. Our results show that it can detect novel objects with a 91% accuracy rate and achieve a 95% recognition rate for known objects. Importantly, it can label novel objects with a 0.71 ARI according to the ground-truth labels.

Our classification result is better than the alternative methods. Although the same Navie Bayes classifier is used to classify known objects detected by isolated forests and GMM, their results are lower than ours. Besides, NNO also provide poorer classification results as it cannot detect known object very well. These results suggest that novelty detectors have an influence on recognition rates, as failure to detect both known and novel objects can result in misclassification. On the other hand, using different classifiers with the same novelty detector yields similar classification results, illustrating the robustness of using mechanical properties as features.

The proposed clustering algorithm achieved the best performance because of the help of the new cluster parameters estimator. Unlike DenStream [31], our method exploits the knowledge of known objects to synthetically create a new cluster when encountering a novel object and update the new cluster when there are enough datapoints in it. This process aligns the cluster's size and position to be close to the ground truth, thus better clustering performance. Besides, the proposed method doesn't need a complete set of data like K-means and DBscan to perform clustering or a predefined number of clusters like K-mean and IOKM [30], which is beneficial for robots learning about new objects in real-world scenarios.

The ARI value with simple regression models as cluster parameter estimators is higher than with randomly generated parameters illustrating the benefit of using the regression model to exploit the known object knowledge to estimate the parameters of the new cluster. On the other hand, using VAE as the estimator results in the lowest values of ARI even though VAE has been successfully used to generate fake samples in visual-based zero-shot learning [32]. This might be the fact that such generative methods require a large number of training samples to learn [28], [33]. In our case, less than 25 trials for each object are in the training set which may cause the VAE model to be underfitting.

While the presented system could successfully recognise known objects and learn to cluster novel objects, some limitations should be acknowledged. First, the current system hyperparameters were tuned by grid search which requires a lot of computational time. This could be addressed by using more efficient optimisation methods. Second, the current system relies only on the initial training data, which can lead to poor parameter estimation for novel classes. To address this, the system should incorporate novel objects in a few-shot learning manner. However, incorrect initial labeling of the novel objects may result in poorer performance, thus more accurate clustering algorithm is needed.

In sum, the experiment results illustrate the potential of the proposed framework using mechanical properties to recognise known objects and incrementally learn novel objects to label them. This is done by first detecting known and novel objects. While the known objects are classified, the novel objects are used to synthetically create clusters awaiting more samples to ensure. It is noteworthy that using knowledge of known objects is useful to help create such clusters rather than without. While the framework successfully recognise and labels objects with various mechanical properties, considering the shape of objects and expanding the framework to be able to manipulate them would be useful in haptic exploration.

REFERENCES

- [1] S. Luo, J. Bimbo, R. Dahiya, and H. Liu, "Robotic tactile perception of object properties: A review," *Mechatronics*, vol. 48, pp. 54–67, 2017.
- [2] P. Dallaire, P. Giguère, D. Émond, and B. Chaib-Draa, "Autonomous tactile perception: A combined improved sensing and bayesian nonparametric approach," *Robotics and Autonomous Systems*, vol. 62, no. 4, pp. 422–435, 2014.
- [3] T. Bhattacharjee, H. M. Clever, J. Wade, and C. C. Kemp, "Multimodal tactile perception of objects in a real home," *IEEE Robotics and Automation Letters*, vol. 3, no. 3, pp. 2523–2530, 2018.
- [4] T. Taunyazov, H. F. Koh, Y. Wu, C. Cai, and H. Soh, "Towards effective tactile identification of textures using a hybrid touch approach," in *2019 International Conference on Robotics and Automation (ICRA)*, 2019, pp. 4269–4275.
- [5] G. Cao, Y. Zhou, D. Bollegala, and S. Luo, "Spatio-temporal attention model for tactile texture recognition," in *2020 IEEE/RSJ International Conference on Intelligent Robots and Systems (IROS)*, 2020, pp. 9896–9902.
- [6] A. Bendale and T. Boulton, "Towards open world recognition," in *2015 IEEE Conference on Computer Vision and Pattern Recognition (CVPR)*, 2015, pp. 1893–1902.
- [7] J. Zheng, W. Li, J. Hong, L. Petersson, and N. Barnes, "Towards open-set object detection and discovery," in *Proceedings of the IEEE/CVF Conference on Computer Vision and Pattern Recognition (CVPR) Workshops*, 2022, pp. 3961–3970.
- [8] Z. Wu, Y. Lu, X. Chen, Z. Wu, L. Kang, and J. Yu, "Uc-owod: Unknown-classified open world object detection," in *Computer Vision – ECCV 2022: 17th European Conference, Tel Aviv, Israel, October 23–27, 2022, Proceedings, Part X*, Tel Aviv, Israel: Springer-Verlag, 2022, 193–210.
- [9] Z. Ma, Y. Yang, G. Wang, X. Xu, H. T. Shen, and M. Zhang, "Rethinking open-world object detection in autonomous driving scenarios," in *Proceedings of the 30th ACM International Conference on Multimedia*, ser. MM '22, Lisboa, Portugal: Association for Computing Machinery, 2022, 1279–1288.
- [10] R. Vareto, S. Silva, F. Costa, and W. R. Schwartz, "Towards open-set face recognition using hashing functions," in *2017 IEEE International Joint Conference on Biometrics (IJCB)*, 2017, pp. 634–641.
- [11] M. Günther, P. Hu, C. Herrmann, *et al.*, "Unconstrained face detection and open-set face recognition challenge," in *2017 IEEE International Joint Conference on Biometrics (IJCB)*, 2017, pp. 697–706.
- [12] G. Salomon, A. Britto, R. H. Vareto, W. R. Schwartz, and D. Menotti, "Open-set face recognition for small galleries using siamese networks," in *2020 International Conference on Systems, Signals and Image Processing (IWSSIP)*, 2020, pp. 161–166.
- [13] D. Bogdoll, M. Nitsche, and J. Zollner, "Anomaly detection in autonomous driving: A survey," in *2022 IEEE/CVF Conference on Computer Vision and Pattern Recognition Workshops (CVPRW)*, Los Alamitos, CA, USA: IEEE Computer Society, 2022, pp. 4487–4498.
- [14] K. Cao, M. Brbić, and J. Leskovec, "Open-world semi-supervised learning," in *International Conference on Learning Representations (ICLR)*, 2022.
- [15] K. J. Joseph, S. Khan, F. S. Khan, and V. N. Balasubramanian, "Towards open world object detection," in *Proceedings of the IEEE/CVF Conference on Computer Vision and Pattern Recognition (CVPR)*, 2021, pp. 5830–5840.
- [16] T. E. Boulton, S. Cruz, A. Dharmija, M. Gunther, J. Henrydoss, and W. Scheirer, "Learning and the unknown: Surveying steps toward open world recognition," *Proceedings of the AAAI Conference on Artificial Intelligence*, vol. 33, no. 1, pp. 9801–9807, 2019.
- [17] K. Liu, Q. Yang, Y. Xie, and X. Huang, "Towards open-set material recognition using robot tactile sensing," in *2023 IEEE International Conference on Robotics and Automation (ICRA)*, 2023, pp. 10 345–10 351.
- [18] H.-M. Yang, X.-Y. Zhang, F. Yin, and C.-L. Liu, "Robust classification with convolutional prototype learning," in *Proceedings of the IEEE Conference on Computer Vision and Pattern Recognition (CVPR)*, 2018.
- [19] Z. Su, K. Hausman, Y. Chebotar, *et al.*, "Force estimation and slip detection/classification for grip control using a biomimetic tactile sensor," in *IEEE-RAS International Conference on Humanoid Robots*, 2015, pp. 297–303.
- [20] A. Ren, C. Qi, F. Gao, X. Zhao, and Q. Sun, "Contact stiffness identification with delay and structural compensation for hardware-in-the-loop contact simulator," *Journal of Intelligent and Robotic Systems*, vol. 86, pp. 1–9, 2017.
- [21] W. J. Stronge, *Impact Mechanics*, 2nd ed. Cambridge University Press, 2018.
- [22] M. Bednarek, P. Kicki, J. Bednarek, and K. Walas, "Gaining a sense of touch object stiffness estimation using a soft gripper and neural networks," *Electronics*, vol. 10, no. 1, 2021.
- [23] K. Yane and T. Nozaki, "Recognition of environmental impedance configuration by neural network using time-series

- contact state response,” in *IEEE International Conference on Advanced Motion Control*, 2022, pp. 426–431.
- [24] P. Uttayopas, X. Cheng, J. Eden, and E. Burdet, “Object recognition using mechanical impact, viscoelasticity, and surface friction during interaction,” *IEEE Transactions on Haptics*, vol. 16, no. 2, pp. 251–260, 2023.
- [25] V. K. Verma and P. Rai, “A simple exponential family framework for zero-shot learning,” in *Machine Learning and Knowledge Discovery in Databases*, M. Ceci, J. Hollmén, L. Todorovski, C. Vens, and S. Džeroski, Eds., Cham: Springer International Publishing, 2017, pp. 792–808.
- [26] D. J. Gauthier, E. Bollt, A. Griffith, and W. A. S. Barbosa, “Next generation reservoir computing,” *Nature Communications*, vol. 12, no. 1, 2021.
- [27] D. Campolo, P. Tommasino, K. Gamage, J. Klein, C. M. Hughes, and L. Masia, “H-man: A planar, h-shape cabled differential robotic manipulandum for experiments on human motor control,” *Journal of Neuroscience Methods*, vol. 235, pp. 285–297, 2014.
- [28] Z. Abderrahmane, G. Ganesh, A. Crosnier, and A. Cherubini, “A deep learning framework for tactile recognition of known as well as novel objects,” *IEEE Transactions on Industrial Informatics*, vol. 16, no. 1, pp. 423–432, 2020.
- [29] T. Mensink, J. Verbeek, F. Perronnin, and G. Csurka, “Distance-based image classification: Generalizing to new classes at near-zero cost,” *IEEE Transactions on Pattern Analysis and Machine Intelligence*, vol. 35, no. 11, pp. 2624–2637, 2013.
- [30] A. Abernathy and M. E. Celebi, “The incremental online k-means clustering algorithm and its application to color quantization,” *Expert Systems with Applications*, vol. 207, p. 117927, 2022.
- [31] F. Cao, M. Estert, W. Qian, and A. Zhou, “Density-based clustering over an evolving data stream with noise,” in *SIAM International Conference on Data Mining*, 2006, pp. 328–339.
- [32] V. Verma, G. Arora, A. Mishra, and P. Rai, “Generalized zero-shot learning via synthesized examples,” in *2018 IEEE/CVF Conference on Computer Vision and Pattern Recognition (CVPR)*, Los Alamitos, CA, USA: IEEE Computer Society, 2018, pp. 4281–4289.
- [33] Z. Abderrahmane, G. Ganesh, A. Crosnier, and A. Cherubini, “Haptic zero-shot learning: Recognition of objects never touched before,” *Robotics and Autonomous Systems*, vol. 105, pp. 11–25, 2018.